Metallurgy and Foundry Engineering – Vol. 42, 2016, No. 2, pp. 87–94
http://dx.doi.org/10.7494/mafe.2016.42.2.87

Krzysztof Ziewiec, Mirosława Wojciechowska, Marcin Jasiński, Dariusz Mucha, Marcin Lis

Microstructure and phase composition of the Ni-Si-B-Ag-based plasma spray deposit

Mikrostruktura i skład fazowy natryskiwanego plazmowo stopu na osnowie niklu, krzemu, boru i srebra

Abstract
The aim of this work is to study the possibility of obtaining an amorphous-crystalline composite starting from Ni-Si-B-based powder grade 1559-40 and silver powder. The process of plasma spray deposition was performed on a water-cooled copper substrate. The cooling rate was assessed using a mid-wave infrared MWIR camera. The microstructure of the deposit was studied using scanning electron microscope SEM with an energy dispersive spectrometer EDS. Phase identification was performed using X-ray diffraction XRD. The studies confirmed an amorphous-crystalline microstructure of the deposits. The predominant constituent of the microstructure was amorphous regions enriched in Ni, Si, and B, while the other constituent was Ag-rich crystalline inclusions identified as a face-centered cubic fcc.

Keywords: amorphous/crystalline composite, plasma spray, mid wave infrared (MWIR) camera, scanning electron microscope (SEM), X-ray diffraction (XRD)

Streszczenie
Celem pracy było zbadanie możliwości uzyskania kompozytu amorficzno-krystlicznego przy wykorzystaniu proszku na osnowie niklu, krzemu i boru gatunku 1559-40 oraz proszku srebra. Proces natryskiwania plazmowego przeprowadzono na płytce miedzianej chłodzonej wodą. Szybkość chłodzenia oszacowano za pomocą kamery termowizyjnej pracującej w zakresie środkowej podczerwieni. Mikrostruktura stopu uzyskanego po natrysku była badana za pomocą skaningowego mikroskopu elektronowego SEM wyposażonego w spektrometr z dyspersją energii promieniowania rentgenowskiego. Identyfikację fazową przeprowadzono przy użyciu dyfrakcji rentgenowskiej XRD. Badania potwierdziły występowanie amorficzno-krystalicznej mikrostruktury

Krzysztof Ziewiec Associate Professor Ph.D. Eng., Mirosława Wojciechowska M.Sc. Eng., Marcin Jasiński M.Sc. Eng.: Pedagogical University of Krakow, Institute of Technology, Faculty of Mathematics, Physics and Technical Science, Krakow, Poland; **Dariusz Mucha Ph.D.:** Jerzy Haber Institute of Catalysis and Surface Chemistry Polish Academy of Sciences; **Marcin Lis M.Sc. Eng.:** Institute of Non Ferrous Metals, Gliwice, Poland; kziewiec@up.krakow.pl

w otrzymanych powłokach. Dominującym składnikiem mikrostruktury były obszary bogate w nikiel, krzem i bor, jednak obserwowano także krystaliczne wtrącenia srebra o strukturze regularnej ściennie centrowanej.

Słowa kluczowe: kompozyt amorficzno-krystaliczny, natryskiwanie plazmowe, kamera termowizyjna średniej podczerwieni, SEM, dyfrakcja rentgenowska

1. Introduction

Metallic glasses have been recently considered for use as structural materials with outstanding properties such as high strength, excellent wear resistance, and special electric and magnetic properties [1]. However, a major problem of their applications is the rapid formation of localized shear bands and eventual damaging, which causes the abrupt deterioration of ductility, especially upon uniaxial tension [2]. A number of methods are used for the production of metallic glasses and glass-matrix composites, such as melt spinning [3], high-pressure die casting [4], water quenching [5], and suction casting [6]. However, in the case of the above-mentioned methods, obtaining applicable massive elements requires huge glass-forming ability. Manufacturing the massive amorphous matrix composites containing immiscible elements is also very difficult or impossible by use of these methods. These disadvantages, fortunately, can be avoided by using a plasma spraying method, which provides a high quenching rate of the molten alloy (typically 10^5–10^7 K/s) [7]. Besides, this method is perfectly suitable for preparing amorphous coatings on elements of various shapes and sizes. The aim of the present work is to produce a plasma-sprayed composite starting from Ni-Si-B-based powder (grade 1559-40) and silver powder and studying its microstructure and phase composition.

2. Experimental

In this investigation, copper plates with dimensions of 80 mm × 40 mm × 5 mm cooled at the bottom by water circulating through a pipe soldered to the plate were used as the substrate. The plates were plasma sprayed using a mixture of two powders. The major constituent (i.e., 95 wt% of the mixture) consisted of Ni-Si-B-based 1559-40 grade powder produced by Höganäs (particle diameter 53–150 μm), and 5 wt% of the mixture consisted of Ag powder (particle diameter <63 μm) produced by INMET. The chemical composition and particle size specification are provided in Table 1. The spraying process was carried out with the application of automated AP-50 plasma installation by Flame Spray Technologies, which cooperates with an F4 plasma torch and PF-50 powder feeder. The torch and water-cooled substrate are presented in Figure 1. The plasma-forming gas flow rates were 54 l/min for Ar and 9 l/min for H_2. Carrier gas transporting powder to the plasma stream was Ar flowing at a rate of 4.2 l/min. The current was 530 A, torch-sample distance: 120 mm, and velocity of sample movement: 0.3 m/s.

Table 1. Specification of 1559–40 powder

Particle size [μm]	Chemical composition [wt %]				
	C	Si	B	Fe	Ni
53–150	≤0.06	3.0	2.9	0.2	balance

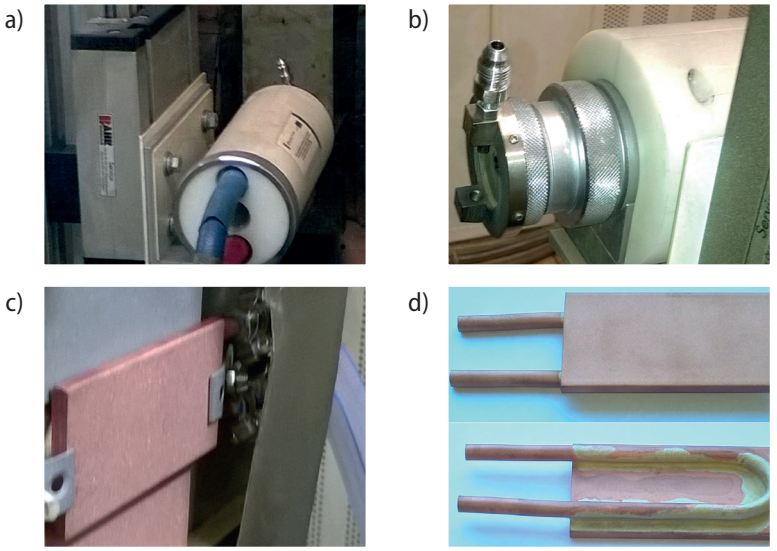

Fig. 1. Plasma-spray deposition on water-cooled copper plate: a); b) plasma torch; c) copper plate mounted on a moving table; d) substrate: copper plate and copper U-shaped pipe soldered using Ag-base solder

The spraying process was observed and recorded using an FLIR SC7650 mid-wave IR-camera. The cross-section microstructure of the plasma-sprayed deposit was investigated using a JEOL 6610 SEM equipped with EDS. X-ray diffraction was performed on a Rigaku Miniflex-2 diffractometer using CuKα radiation filtered by an LiF bent single crystal on the detector side. Scattering angle 2Θ varied between 30° and 70° degrees.

3. Results and discussion

Figure 2 presents the IR snapshot sequence of the substrate mounted on a table traveling in front of the plasma-spraying torch. Figure 3 shows the time plot of the temperature changes during the subsequent passes of the substrate. During the movement that corresponds to the apparent temperature change marked in Figure 3a as "A" is presented in Figure 3b as a plot with an extended time scale, and a temperature arrest is observed below 950°C.

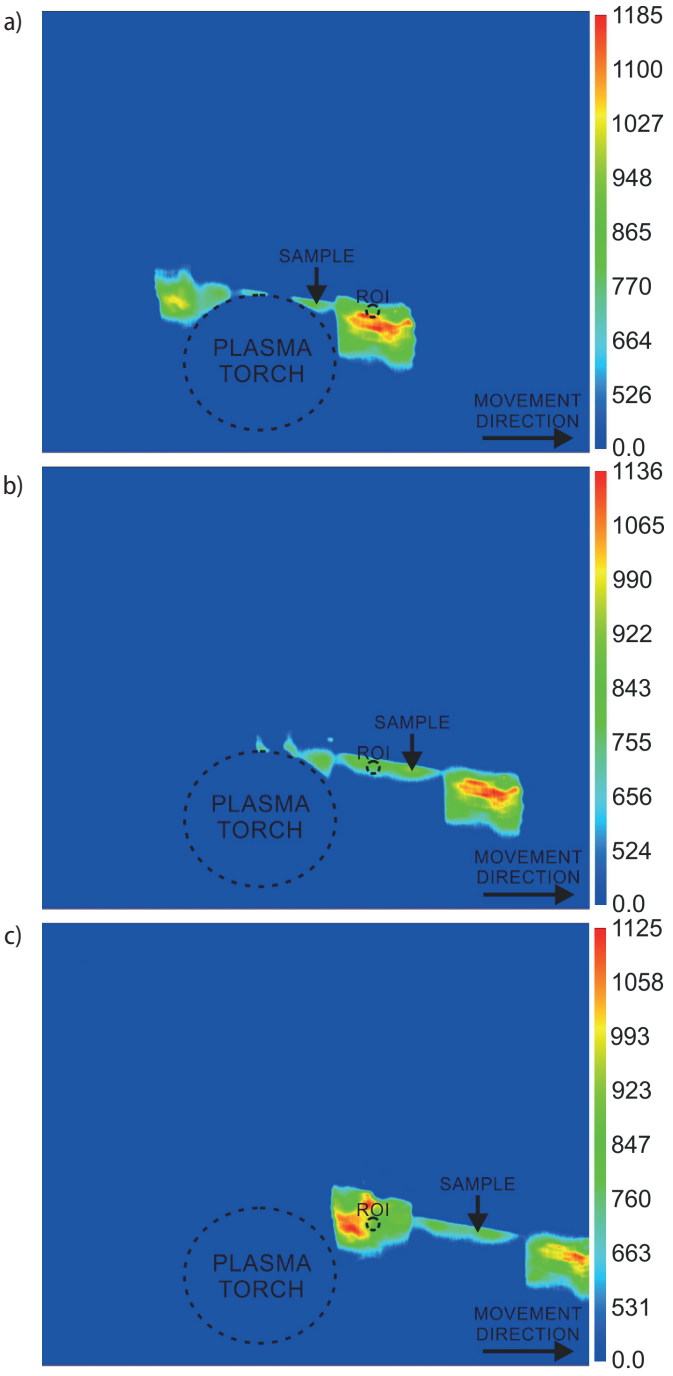

Fig. 2. Sequence of IR images; a), b), c) showing temperature distribution at the substrate

This segment of the curve can be attributed to the crystallization temperature of the Ag-rich phase. The equilibrium crystallization temperature of silver is 961.78°C. A slightly lower value (ca. 950°C) observed in the present study can be due to undercooling and alloying of the silver in a liquid state. Defining the cooling rate is very difficult in conditions of cyclic spraying of highly superheated metallic droplets; however, the heating rate until crystallization of the silver Ag-rich constituent of the layer is ca. $1.6 \cdot 10^3$ K/s. Cooling to a lower temperature is slower (ca. $3.7 \cdot 10^2$ K/s), due to the thermal diffusivity of the deposit and the latent heat flowing from the crystallizing constituents of the Ni-Si-B alloy.

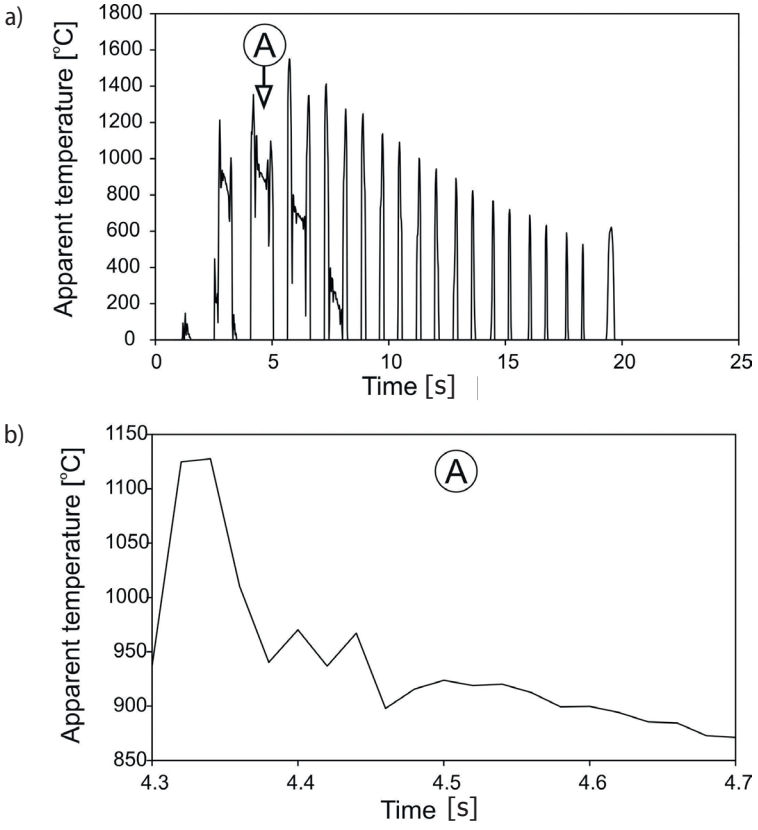

Fig. 3. Time plot of the apparent temperature changing at the ROI (region of interest) marked by the circle region in Figure 2: a) dependence showing several passes of the table in front of the plasma torch; b) dependence of the temperature change from the segment of measurement indicated by the "A" arrow

Figure 4 shows the microstructure observed on the cross-section of the deposit. Gray color matrix (Fig. 4a) is enriched with Ni (Fig. 4c). On the other hand, the brighter

flake-like inclusions are enriched with Ag (Fig. 4b). This observation is consistent with the high positive enthalpy of mixing $\Delta H^{mix}_{\{NiAg\}} = +15\,kJ/mol$ [8]. Si is distributed more homogeneously. Nevertheless, Figure 4d shows a lower number of counts in the locations of Ag-based flakes. The content of B was not analyzed; but due to a high positive enthalpy of mixing $\Delta H^{mix}_{\{AgB\}} = +5\,kJ/mol$ [9], it is likely that there is a low boron content in the Ag-rich flakes. The mixing enthalpies for Ni-B and Ni-Si are $\Delta H^{mix}_{\{NiB\}} = -9\,kJ/mol$ and $\Delta H^{mix}_{\{NiSi\}} = -23\,kJ/mol$ [8], respectively. Therefore, Ni-rich regions are probably highly enriched by boron.

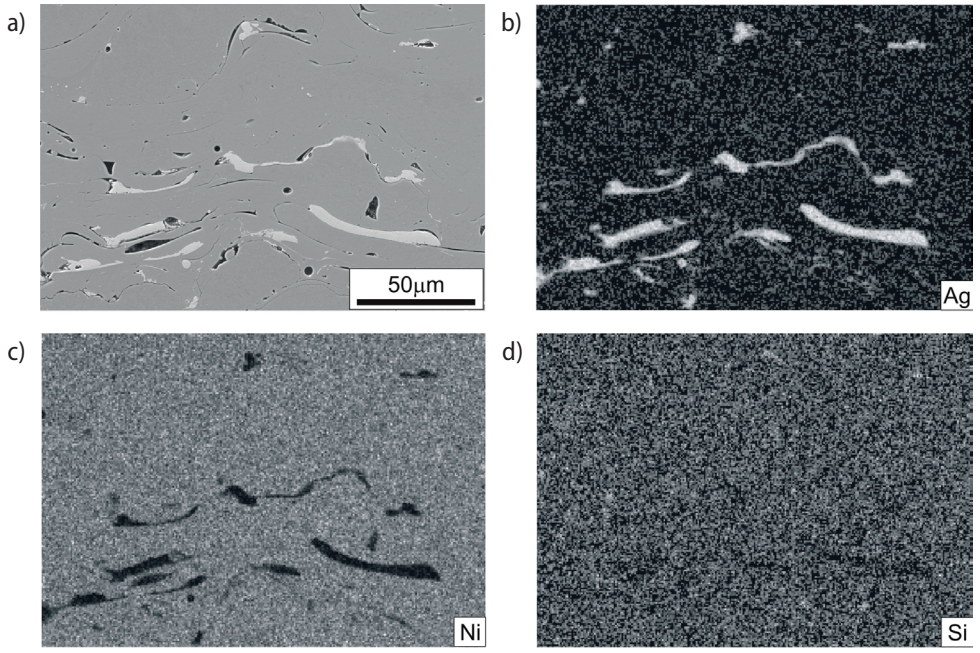

Fig. 4. Cross-section microstructure of the plasma-sprayed deposit and EDS analysis: a) SEM image; b) Ag distribution; c) Ni distribution; d) Si distribution

XRD presented in Figure 5 is complex, and as much as five crystalline phases can be attributed to the sample isomorphic with the following phases: Ag – face centered cubic FCC PDF NO.: 04-004-8504, Ni – FCC PDF NO.: 04-010-6148, Ni_3Si – FCC PDF. NO: 04-001-3293. However, all of the peaks from the crystalline phases identified in the diffraction are relatively weak. Background intensity between 30° and 50° is elevated. This could be due to the presence of the amorphous phase in the sample. Therefore, the cooling rate occurring during plasma deposition could be sufficient for at least partial amorphization of the product.

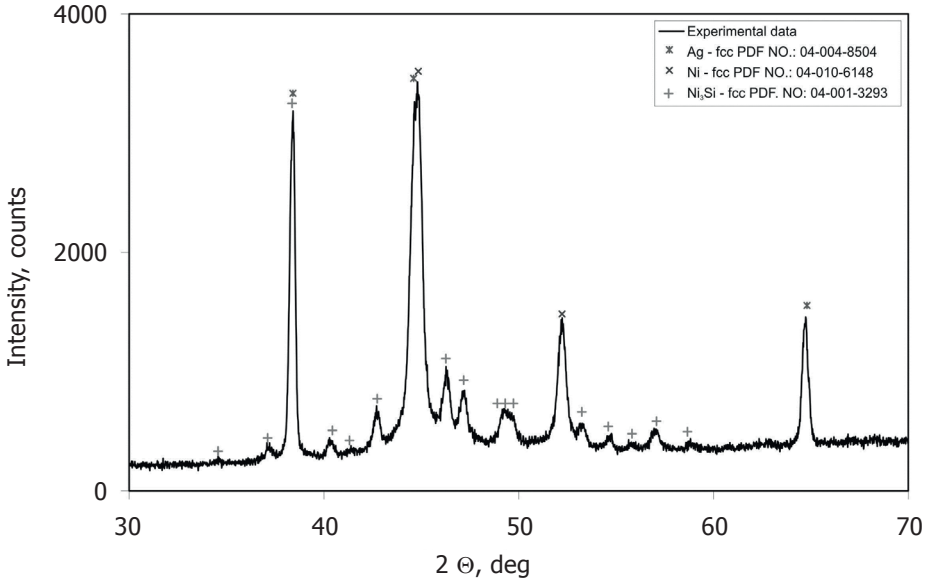

Fig. 5. XRD from the bottom of the plasma-sprayed deposit; markers under the experimental data present the positions of the peaks for the identified crystalline phases

4. Summary

In spite of the difficulty in defining the cooling conditions, the cooling rate until crystallization of the Ag-rich constituent was estimated at a level of ca. $1.6 \cdot 10^3$ K/s. However, further cooling of the deposit is slower (ca. $3.7 \cdot 10^2$ K/s) due to the relatively low thermal diffusivity of the material and the latent heat flowing from the crystallizing constituents (i.e., the Ni-Si-B matrix and Ag-based precipitates). However, these cooling conditions are obviously sufficient for enabling partial amorphization of the Ni-Si-B-rich matrix. This interpretation of the IR-camera observations is supported by the SEM study and XRD observation, because the microstructure of the layer containing highly alloyed Ni-Si-B-rich partially amorphous matrix and crystalline Ag-rich flake-like inclusions poorly alloyed by Ni, Si, and B.

Acknowledgements

The study was supported by National Science Center (NCN) under project No. 2012/05/B/ST8/02644.

References

[1] Löffler J.F.: Bulk metallic glasses. Intermetallics, 11 (2003), 529–540

[2] Tian L., Shan Z.-W., Ma E.: Ductile necking behavior of nanoscale metallic glasses under uniaxial tension at room temperature. Acta Materialia, 61 (2013), 4823–4830

[3] Budhani R.C., Goel T.C., Chopra K.L.: Melt spinning for preparation of metallic glasses. Bulletin of Materials Science, 4, 5 (1982), 549–561

[4] Borowski A., Guwer A., Gawlas-Mucha A., Babilas R., Nowosielski R.: Fabrication of Mg-based bulk metallic glasses by pressure die casting method. Indian Journal of Engineering & Materials, 21 (2014), 259–264

[5] Zhang X., Zhang Y., Chen X., Chen G.: Bulk metallic glass rings prepared by a modified water quenching method. International Journal of Minerals, Metallurgy and Materials, 16, 1 (2009), 108–111

[6] Kozieł T., Matusiewicz P., Kopyściański M., Zielińska-Lipiec A.: Estimation of the cooling rate in 3 mm suction-cast rods based on the microstructural features. Metallurgy and Foundry Engineering, 39, 2 (2013), 7–14

[7] Kobayashi A., Yano S., Kimura H., Inoue A.: Fe-based metallic glass coatings produced by smart plasma spraying process. Materials Science and Engineering B, 148 (2008), 110–113

[8] Boer F.R., Boom R., Mattens W.C.M., Miedema A.R., Niessen A.K.: Nickel. In: Boer F.R., Boom R., Mattens W.C.M., Miedema A.R., Niessen A.K.: Cohesion and structure, vol. 1: Cohesion in metals. Transition metal alloys. Elsevier Science 1988, Amsterdam, 291–322

[9] Takeuchi A., Inoue A.: Mixing enthalpy of liquid phase calculated by Miedema's scheme and approximated with sub-regular solution model for assessing forming ability of amorphous and glassy alloys. Intermetallics, 18 (2010), 1779–1789